Astrodynamics Vol. 7, No. 4, 445–453, 2023 https://doi.org/10.1007/s42064-023-0171-7

Self-induced collision risk of the Starlink constellation based on long-term orbital evolution analysis

Wei Zhang (✉), Xiuhong Wang, Wen Cui, Zhi Zhao, and Sirui Chen

Xi'an Satellite Control Center, Xi'an 710043, China

ABSTRACT

The deployment of mega constellations has had a significant effect on the compounding space debris environment, increasing the number of on-orbit objects in all conditions and damaging the stability of the space debris environment. The increased density of space objects is associated with an increased risk of on-orbit collisions. Collision risk exists not only between a mega constellation and the space debris environment but also inside a mega constellation. In this study, we used the Starlink constellation to investigate the self-induced collision risk caused by malfunctioning satellites. First, we analyzed the conjunction condition between malfunctioning and operative satellites based on long-term orbital evolution characteristics. The collision probability was then calculated based on the conjunction analysis results. The results show that malfunctioning satellites in Phase 1 cause an 86.2% self-induced collision probability based on a malfunctioning rate of 1%, which is close to the collision probability caused by objects larger than 6 cm during five years of service. Therefore, self-induced collisions are another important risk factor for the Starlink constellation.

KEYWORDS

Starlink constellation
orbit evolution
self-induced collision
collision probability

Research Article

Received: 14 February 2023
Accepted: 22 June 2023

1 Introduction

Spacecraft collision avoidance and space traffic management have always been crucial concerns for space safety. According to a space environment report released on the Space-Track website, there are currently approximately 26,000 space objects that can be detected in space [1], representing an increase of approximately 40% over the past decade. In addition, there are a vast number of space debris and particles below the centimeter level. With the exception of breakup events, the rapid deployment of low-Earth orbit (LEO) mega constellations, such as SpaceX's Starlink constellation, which is intended to provide global Internet access by deploying nearly 42,000 satellites, has become another important reason for the sharp increase in the number of space objects. As of March 1, 2023, SpaceX has launched a total of 4000 Starlink satellites, which is almost equal to the number of all other active spacecraft in orbit. The increased density of space objects is one of the main causes of the increased risk of on-orbit collisions. These collisions may cause a large catastrophe, such as the Kessler Syndrome, rendering the near-Earth space completely unusable [2]. In recent years, the deployment of the Starlink constellation has caused the frequent occurrence of high-risk conjunctions between the Starlink satellites and other spacecraft [3]. In September 2019, the European Space Agency (ESA) maneuvered the Aeolus satellite to avoid collision with Starlink-44 [4]. In July and October 2021, the Chinese Space Station (CSS) executed two emergency maneuvers to mitigate the risk of collisions with the Starlink satellites [5].

The collision risk caused by mega constellations, such as Starlink, has been studied in depth [6–9]. Le May *et al.* [9] used the MASTER model to study the probability of external collisions for mega constellations in the current space debris environment and indicated that strict postmission disposal was the key to reducing the side effects of mega constellations in the near-Earth space environment. In addition to the collision risks between the mega constellations and the external environment,

✉ colagrape@163.com

collision risks inside the mega constellations also exist. Lewis *et al.* [10] reported that approximately 25% of the collision risks in a mega constellation are self-induced, that is, caused by the interior of the constellation. Hu *et al.* [11–13] studied the long-term evolution of a constellation configuration and stated that the initial orbit deviation breaks the stability of the constellation configuration under the influence of perturbations, resulting in changes in the relative positions of the satellites within the constellation. To maintain the orbital altitude of the Starlink constellation, the satellite must perform frequent orbital maneuvers to counteract the dissipation effect caused by atmospheric drag. Based on a preliminary analysis of two-line elements (TLEs), the Starlink satellite, which operates at an altitude of approximately 550 km, must implement a small maneuver every 3–4 days. In the case of frequent maneuvers, the long-term effects of initial orbital deviations between satellites can be ignored. However, the satellites in the constellation may suddenly suffer malfunctions, which will change the constellation configuration. For example, on September 1, 2022, the Starlink constellation had a total of 2940 on-orbit satellites, of which 24 were suspected to have sudden on-orbit faults and failed to deorbit in time, with an estimated malfunctioning rate of nearly 1%. The identifiers of these 24 satellites in the TLE were "U". By contrast, an operative Starlink satellite was identified with a "C", indicating that these 24 satellites failed. Thus, the self-induced collision risk within the constellation caused by malfunctioning satellites requires further investigation.

This study aims to analyze the self-induced collision risk of the Starlink constellation caused by malfunctioning satellites. First, the long-term orbital evolution characteristics of a Starlink satellite were analyzed using orbit perturbation theory. On this basis, the conjunction between the malfunctioning and operative satellites in the same or different orbital planes was studied. Finally, the collision probability caused by the malfunctioning satellites was presented, which can be used as a reference for future space traffic management.

2 Stability analysis of the Starlink constellation's structure

The main orbital perturbations for the Starlink constellation are the Earth's nonspherical gravity and atmospheric drag perturbation. The J_2 zonal harmonics, which is the major term of the Earth's nonspherical gravity, affects the orbital plane (mainly the right ascension of ascending node (RAAN), Ω) and phase angle $\theta = \omega + M$ of the satellite but does not affect the long-term changes in the orbital altitude and shape. Note that ω and M are arguments for the perigee and mean anomaly, respectively. The atmospheric drag mainly affects the orbital altitude and shape of the satellite but does not affect the orbital plane.

The long-term effects of the Earth's J_2 perturbation and atmospheric drag acting on an orbit are [14]:

$$\begin{cases} \dot{a} = -B\rho v\left(\frac{a}{1-e^2}\right) \\ \qquad \cdot \left[1 + 2e\cos f + e^2 - \omega_{\mathrm{E}}\cos i\sqrt{\frac{a^3(1-e^2)^3}{\mu}}\right] \\ \dot{e} = -B\rho v\Bigg\{\cos f + e - \frac{\omega_{\mathrm{E}}\cos i\sqrt{a^3(1-e^2)^3}}{2(1+e\cos f)^2} \\ \qquad \cdot [2(e+\cos f) - e\sin^2 f]\Bigg\} \\ \dot{i} = 0 \\ \dot{\Omega} = -\frac{3J_2R_e^2}{2p^2}n\cos i \\ \dot{\omega} = \frac{3J_2R_e^2}{4p^2}n(4 - 5\sin^2 i) \\ \dot{M} = n\left[1 + \frac{3J_2R_e^2}{4p^2}(2 - 3\sin^2 i)\sqrt{1-e^2}\right] \end{cases} \tag{1}$$

where a, e, i, Ω, ω, and M are the Keplerian orbital elements of the satellite; B is the ballistic coefficient of the satellite, defined as the product of the atmospheric drag coefficient and area-to-mass ratio (AMR); ρ is the atmospheric density; and v is the satellite's motion velocity relative to the atmosphere. Furthermore, ω_{E} is the Earth's rotation rate; μ is the Earth's gravitational constant; R_{e} is the Earth's mean equatorial radius; n is the satellite's mean motion; and p is the orbit's semilatus rectum.

The orbital altitude and inclination of Starlink satellites within the same shell are similar, and the eccentricity is close to zero. Equation (1) shows that the change rate of RAAN ($\dot{\Omega}$) and the phase angle ($\dot{\theta}$) for two satellites in the same shell are similar. Hence, the relative position between these two satellites theoretically remains unchanged, and the constellation configuration is stable. However, owing to the deviation of the initial orbit between the satellites, there are differences in $\dot{\Omega}$ and $\dot{\theta}$ which leads to a drift in the constellation configuration over time. Assuming that the initial orbital deviation between the two satellites is Δa, Δe, Δi, $\Delta\Omega$, $\Delta\omega$, and

ΔM, the increments of $\dot{\Omega}$ and $\dot{\theta}$ (denoted as $\Delta\dot{\Omega}$ and $\Delta\dot{\theta}$, respectively), caused by the orbital initial deviation are expressed as

$$\Delta\dot{\Omega} = -\frac{7\dot{\Omega}}{2a}\Delta a + \frac{4ae\dot{\Omega}}{R_e p}\Delta e - \frac{\sin i\dot{\Omega}}{\cos i}\Delta i \tag{2}$$

$$\Delta\dot{\theta} = -\frac{7\dot{\theta}}{2a}\Delta a + \frac{ae}{R_e p}\left[\frac{3J_2}{4p^2}n(4-5\sin^2 i)+3\dot{\theta}\right]\Delta e - \frac{3J_2}{4p^2}n\left(5+3\sqrt{1-e^2}\right)\sin 2i\Delta i \tag{3}$$

Chen *et al.* [12] analyzed the influence of the initial orbit deviation on the constellation configuration and stated that the lower the orbital altitude, the greater the influence of the semimajor axis deviation on the RAAN and phase angle drift; for low-orbit satellites, a semimajor axis deviation of the order of 10 m causes a phase angle drift of 4° in a year. To maintain the constellation configuration, orbit control of a satellite is required. Common strategies include absolute and relative configuration preservation. Absolute configuration preservation is used to maintain the absolute position of all satellites in the constellation in a certain coordinate system and is typically necessary to compensate for the orbital altitude decay caused by atmospheric drag and the phase drift caused by J_2 perturbation terms. Relative configuration maintenance requires only the relative position relationship between satellites to be maintained [15]. Because the deployment and operation of the Starlink constellation have rather high requirements for orbital altitude, it is not difficult to see from frequent orbit maintenance that the absolute configuration maintenance strategy is adopted. Orbital maneuvers are performed every 3–4 days for Starlink satellites operating at an altitude of approximately 550 km. In the case of frequent maneuvers, the long-term effects of initial orbital deviations between satellites can be ignored. However, Starlink satellites may suffer sudden faults with a malfunctioning rate of approximately 1%. These malfunctioning satellites cannot maintain a safety gap relative to the other satellites, which may pose a collision threat to the operative satellites.

3 Conjunction analysis between malfunctioning and operative satellites

3.1 Starlink constellation configuration

The orbit distribution of the satellites in Phase 1 based on the deployment plan of the Starlink constellation is listed in Table 1.

Table 1 Orbit distribution of the Starlink satellites (Phase 1)

Orbital shell	Orbital planes	Satellites in each plane	Altitude (km)	Inclination (°)
Shell 1	72	22	550	53
Shell 2	72	22	540	53.2
Shell 3	36	20	570	70
Shell 4	6	58	560	97.6
Shell 5	4	43	560	97.6

As shown in Table 1, there are 4408 satellites in Phase 1 divided into five orbital shells. In addition, there are 7518 satellites in the ultralow orbit shells in Phase 1, with an orbital altitude of approximately 350 km. Owing to the short lifetime of uncontrolled satellites at this altitude, these satellites are outside the scope of this study.

3.2 Conjunction analysis between satellites in the same orbital plane

Compared to the operative satellite, the difference in the motion of the malfunctioning satellite is exhibited as the orbital decay caused by atmospheric drag, which leads to a difference in the mean motion and eventually a difference in the change rate of the RAAN and phase angle. If only the mean motion is considered, the orbital altitude of the malfunctioning satellite decreases, which does not pose a collision risk to other satellites in the same orbital plane. However, the actual orbital motion of the satellite undergoes periodic term changes. In the case of small eccentricity, the first-order periodic term of the semimajor axis and the eccentricity that causes the altitude change of the satellite are expressed as

$$\Delta a_{\mathrm{s}} = \frac{3J_2}{2a}\sin^2 i\cos(2f+2\omega) \tag{4}$$

$$\Delta e_{\mathrm{s}} = \frac{3J_2}{4a^2}\left[(2-3\sin^2 i)\cos f + \sin^2 i\left(3\cos f\cos(2f+2\omega)-\cos(f+2\omega) - \frac{1}{3}\cos(3f+2\omega)\right)\right] \tag{5}$$

$$\Delta a_{\mathrm{l}} = 0, \quad \Delta e_{\mathrm{l}} = 0 \tag{6}$$

where Δa_{s} and Δe_{s} represent the first-order short-periodic terms of the semimajor axis and the eccentricity, respectively; Δa_{l} and Δe_{l} are the first-order long-periodic terms of the semimajor axis and the eccentricity,

respectively. For LEO objects, the first-order short-periodic term of the semimajor axis varies by approximately $10\sin^2 i$ km and that of eccentricity generally varies by less than 0.001. The variation amplitude of the perigee and apogee altitudes of the satellite can be approximately expressed as

$$\Delta H = a\Delta e_{\mathrm{s}} + \Delta a_{\mathrm{s}} \tag{7}$$

Therefore, the orbital altitude variation range of a single LEO satellite is approximately $(7 + 10\sin^2 i)$ km, where 7 km and $10\sin^2 i$ km are caused by the short-periodic variations of eccentricity and the semimajor axis, respectively. To avoid collisions between satellites, the orbital decay of the malfunctioning satellite should be twice the orbital altitude variation range of a single LEO satellite, that is, $(20\sin^2 i + 14)$ km, which is approximately 27 km for a Starlink satellite with a 53° inclination and 34 km for a 97.6° inclination.

The change rate of the semimajor axis and the phase angle of the malfunctioning satellite are also time-dependent, whereas the semimajor axis of an operative satellite in orbit can be considered unchanged with only the phase angle changed. When the eccentricity is close to zero, the differences in the change rate of the semimajor axis and the phase angle of the two satellites are

$$\Delta\dot{a} = -B_{\mathrm{u}}\rho v a_{\mathrm{u}}\left(1 - \omega_{\mathrm{E}}\cos i\sqrt{\frac{a_{\mathrm{u}}^3}{\mu}}\right) \tag{8}$$

$$\Delta\dot{\theta} = n_{\mathrm{u}} - n_{\mathrm{o}} + \frac{3}{2}J_2 R_{\mathrm{e}}^2\left(3 - 4\sin^2 i\right)\left(\frac{n_{\mathrm{u}}}{a_{\mathrm{u}}^2} - \frac{n_{\mathrm{o}}}{a_{\mathrm{o}}^2}\right) \tag{9}$$

where n_{o} is the mean motion of the operative satellite, and B_{u}, a_{u}, and n_{u} represent the ballistic coefficient, semimajor axis, and mean motion of the malfunctioning satellite, respectively.

Taking Shell 1 of the Starlink constellation as an example, the normal orbit of the satellite is approximately 550 km in altitude with a 53° inclination. There are 72 orbital planes in this shell, with 22 satellites in each plane. Assuming that the satellites are uniformly deployed, the phase-angle difference between two adjacent satellites is approximately 16.36°. In the case of a moderate atmospheric environment, the changes in the semimajor axis and the phase angle of the malfunctioning satellite with different AMRs over time are shown in Figs. 1 and 2. The phase angle drift of the satellite with an AMR of 0.01 m^2/kg reaches 16.36° after approximately 32.9 days, catching up with the adjacent operative satellite in front. Simultaneously, the orbital altitude of the malfunctioning satellite decreases by approximately 0.8 km. Furthermore, the phase angle drift reaches 32.72° after approximately another 13.6 days, catching up with the previously occupied operative satellite again. At this time, the orbital altitude of the malfunctioning satellite decreases by approximately 1.2 km. Moreover, an orbital decay of 27 km would take more than two years. Meanwhile, the phase angle drift of the satellite with an AMR of 0.02 m^2/kg reaches 16.36° after 23.2 days, catching up with the adjacent operative satellite in front. Simultaneously, the orbital altitude of the malfunctioning satellite decreases by approximately 1.2 km. Furthermore, the phase angle drift reaches 32.72° after approximately another 9.6 days, catching up with the previously occupied operative satellite again. At this time, the orbital altitude of the malfunctioning satellite decreases by approximately 1.7 km. Moreover, an orbital decay of 27 km would take approximately one year. For the satellite with an AMR of 0.05 m^2/kg, its phase angle drift reaches 16.36° after 14.7 days, catching up with the adjacent operative satellite in front. Simultaneously, the orbital altitude of the malfunctioning satellite decreases by approximately 1.9 km. Furthermore, the phase angle drift reaches 32.72° after approximately six days, catching up with the previously occupied operative satellite again. At this time, the orbital altitude of the malfunctioning satellite decreases by approximately 2.7 km. Moreover, an orbital decay of 27 km would take approximately 0.5 years. Thus, the lower the orbital altitude of the satellite, the faster the orbit decays; the shorter the time required to catch up with the adjacent satellite in front, the smaller the number of conjunctions.

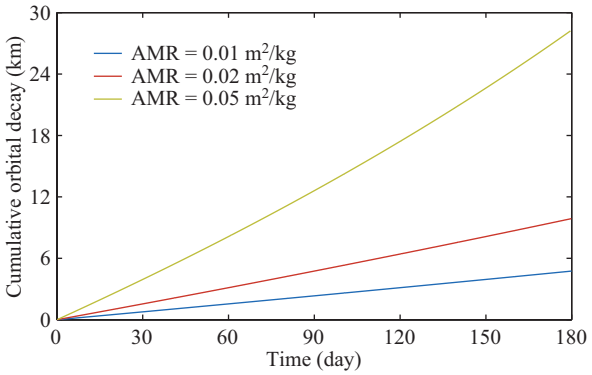

Fig. 1 Orbital decay of the malfunctioning satellites in Shell 1.

One malfunctioning and two normally operating Starlink satellites in orbit were simulated and analyzed.

Table 2 Orbital parameters of malfunctioning and normal Starlink satellites

Satellite	Altitude (km)	Eccentricity	Inclination (°)	RAAN (°)	Phase angle (°)	AMR (m^2/kg)
Malfunction satellite	547.5	0.0001	53.05	184.05	201.28	0.02
Operative satellite 1	547.5	0.0001	53.05	184.05	217.64	0.02
Operative satellite 2	547.5	0.0001	53.05	184.05	234.00	0.02

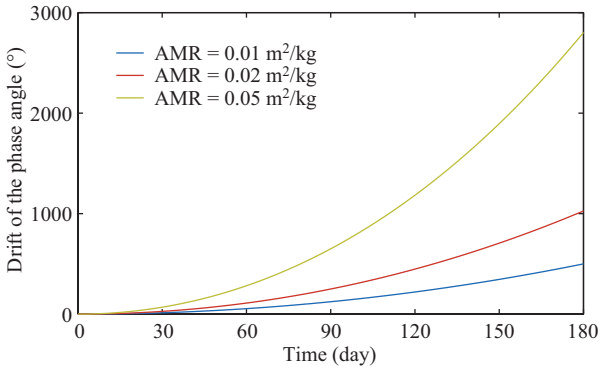

Fig. 2 Phase angle drift of the malfunctioning satellites in Shell 1.

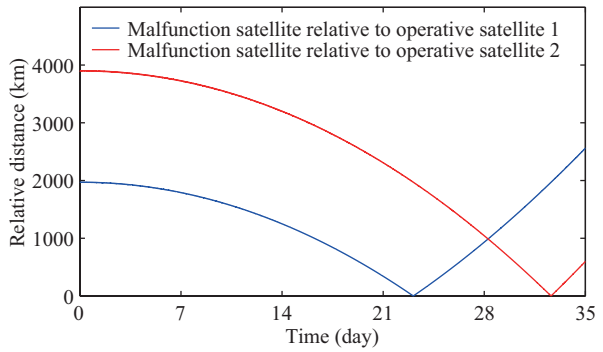

Fig. 3 Conjunctions between one malfunctioning and two operative satellites.

The orbital parameters are listed in Table 2. The conjunctions between the malfunctioning satellite and the two normal satellites are shown in Fig. 3.

As shown in Fig. 3, the malfunctioning satellite approaches operative satellite 1 after approximately 23.1 days, with the closest distance being approximately 1.9 km. Furthermore, it approaches operative satellite 2 after approximately 32.7 days, with the closest distance being approximately 3.0 km. Both of these scenarios have rather high collision risks. Nevertheless, the Starlink satellites in the same orbital plane run in the same direction, and the relative velocity is small (approximately 5 m/s for a 10 km difference in the semimajor axis). Even if a collision occurs, it will not cause catastrophic satellite disintegration (i.e., an energy-to-mass ratio greater than 40 kJ/kg) [16].

3.3 Conjunction analysis between satellites in different orbital planes

The relative distance r_{rel} between the operative and malfunctioning satellites can be expressed as [17]:

$$r_{\mathrm{rel}}^2 = r_{\mathrm{o}}^2 + r_{\mathrm{u}}^2 - 2r_{\mathrm{o}}r_{\mathrm{u}}\cos\gamma \tag{10}$$

where r_{o} and r_{u} are the geocentric distances between the operative and malfunctioning satellites, respectively, and γ is the geocentric angle between the two satellites. The initial phase angle between the two satellites is assumed to be θ_0. For a near-circular orbit satellite, the first-order expression of r_{rel} can be written as

$$r_{\mathrm{rel}}^2 = a_{\mathrm{o}}^2 + a_{\mathrm{u}}^2 - 2a_{\mathrm{o}}a_{\mathrm{u}}\cos\gamma \tag{11}$$

$$\cos\gamma = \frac{1}{2}(1+\cos I)\cos\left(n_{\mathrm{o}}t - \int n_{\mathrm{u}}\mathrm{d}t + \theta_0\right) + \frac{1}{2}(1-\cos I)\cos\left(n_{\mathrm{o}}t + \int n_{\mathrm{u}}\mathrm{d}t - \theta_0\right) \tag{12}$$

where I is the included angle of two orbital planes.

$$\cos I = \cos^2 i + \sin^2 i\cos\Delta\Omega \tag{13}$$

where $\Delta\Omega$ is the difference between the RAANs of operative and malfunctioning satellites. The semimajor axis of the operative satellite remains unchanged, whereas that of the malfunctioning satellite continues to decay owing to atmospheric drag, which can be expressed as

$$a_{\mathrm{u}} = a_{\mathrm{o}} + \int \dot{a_{\mathrm{u}}}\mathrm{d}t \tag{14}$$

Taking Shell 1 of the Starlink constellation as an example and assuming that the satellite is uniformly deployed, the difference between the RAANs of the two satellites is $\Delta\Omega = K\Delta\Omega_0$ (K is an integer between 1 and 71) and $\Delta\Omega_0 = 5°$. The AMR of a malfunctioning satellite is assumed to be 0.02 m^2/kg. K takes the value of 1. The changes in r_{rel} under the three conditions with θ_0 values of 8.18°, 24.54°, and 40.9° are shown in Fig. 4.

An increase in orbital decay increases the difference in the mean motion between the malfunctioning and operative satellites and the conjunction frequency. Furthermore, the periodic term of r_{rel} in Eqs. (11) and (12) is $\int n_{\mathrm{u}}\mathrm{d}t$, which is equal to the periodic term in Eq. (9). Thus, the number of conjunctions for satellites in

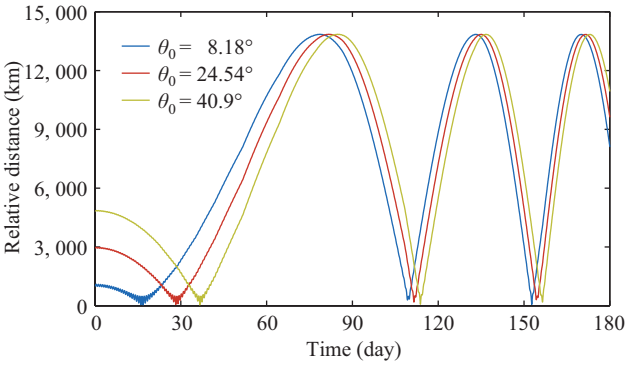

Fig. 4 Conjunctions of satellites in different orbital planes.

different orbital planes is equivalent to that for satellites in the same orbital plane. However, the relative speed of the former is larger, typically exceeding 1 km/s. Once a collision occurs, it inevitably leads to a catastrophic on-orbit breakup. Therefore, the collision between the two satellites in different orbital planes is more harmful.

4 Constellation self-induced collision probability analysis

4.1 Analysis method

The number of collisions caused by the malfunctioning satellite can be calculated by [18]:

$$N = F \cdot A_{\mathrm{c}} \cdot T \tag{15}$$

where F is the flux index; T is the duration of the analysis; and A_{c} is the collision cross-sectional area, which can be computed using the radii of both the impactor and target objects.

$$A_{\mathrm{c}} = \pi(r_{\mathrm{tar}} + r_{\mathrm{imp}})^2 \tag{16}$$

where r_{tar} is the equivalent radius of the target satellite, and r_{imp} is the equivalent radius of the impact satellite.

For space debris, the flux index F can be calculated using a debris model, such as the MASTER model. In this study, we calculated F using the number of conjunctions during the decay of the malfunctioning satellite, as in Eq. (17):

$$F = \frac{N_{\mathrm{ce}}}{t_{\mathrm{D}} \times A_{\mathrm{o}}} \tag{17}$$

where N_{ce} is the number of conjunctions analyzed in Section 3; t_{D} is the time duration when the malfunctioning satellite may threaten the operative satellite, that is, the time of cumulative orbital decay larger than $(20\sin^2 i + 14)$ km; and A_{o} is the occupation cross-sectional area of the malfunctioning satellite, which is determined by the short-periodic term.

Once the flux index F is determined, the Poisson distribution is used to calculate the probability of x collisions as in Eq. (18):

$$P_x = \frac{N^x}{x!}\mathrm{e}^{-N} \tag{18}$$

Therefore, the probability of no collision is

$$P_0 = \mathrm{e}^{-N} \tag{19}$$

The probability of more than one collision is

$$P_{\geqslant 1} = 1 - P_0 = 1 - \mathrm{e}^{-N} \tag{20}$$

4.2 Collision probability results

4.2.1 Number of collisions in the same shell and orbital plane

The Starlink satellite in Shell 1 is used as an example. The AMR of the malfunctioning satellite is assumed to be 0.02 m^2/kg. According to the analysis results above, it takes approximately 400 days for the satellite's orbital altitude to decay by more than 27 km, and the total phase angle drift is approximately 5500° in total. If there are 21 other operative satellites in the same orbital plane, the malfunctioning satellite approaches the operative satellites approximately 321 times. The short-periodic term of the satellite is used to determine the occupied cross-sectional area. The amplitude of the altitude direction is $(20\sin^2 i + 14)$ km, which is 27 km. The value in the transverse direction was determined based on the short-periodic term of the orbital inclination. For the low orbit satellite, the amplitude of the short-period term of inclination is approximately 0.02°, and the transverse direction was 5 km. Therefore,

$$\begin{aligned} F &= \frac{N_{\mathrm{ce}}}{t_{\mathrm{D}} \times A_{\mathrm{o}}} = \frac{321}{400\,\mathrm{d} \times 27\,\mathrm{km} \times 5\,\mathrm{km}} \\ &\approx 2.17 \times 10^{-6}\ \mathrm{m}^{-2}{\cdot}\mathrm{a}^{-1} \end{aligned} \tag{21}$$

We assume that the equivalent radius of the satellite is 2.39 m [6]. According to Eq. (15), the number of collisions between the malfunctioning and operative satellites in the same shell and orbital plane is 1.72×10^{-4}. The number of collisions with other shells is calculated using the same method, and the results are listed in Table 3.

4.2.2 Number of collisions in the same shell but different orbital planes

The Starlink satellite in Shell 1 is considered an example. Assuming that the AMR is 0.02 m^2/kg, a malfunctioning satellite will approach the other 1562 operative satellites in different orbital planes approximately 24,493 times

Table 3 Number of collisions of a single malfunctioning satellite with other operative satellites in the same shell and orbital plane

Shell	Shell 1	Shell 2	Shell 3	Shell 4	Shell 5
Number of collisions	1.72×10^{-4}	1.64×10^{-4}	3.21×10^{-4}	9.24×10^{-4}	6.96×10^{-4}

before the orbital altitude decays by 27 km. The F index is calculated to be 1.62×10^{-4} $\mathrm{m^{-2} \cdot a^{-1}}$, and the number of collisions between the malfunctioning and operative satellites in the same shell but different orbital planes is 0.013. The number of collisions in the other shells is calculated using the same method, and the results are presented in Table 4.

Table 4 Number of collisions of a single malfunctioning satellite with other operative satellites in the same shell but different orbital planes

Shell	Shell 1	Shell 2	Shell 3	Shell 4	Shell 5
Number of collisions	0.013	0.012	0.012	0.005	0.002

4.2.3 Number of collisions between different shells

The collision risks between different shells must be calculated separately based on the height relationship between the shells. For example, considering the collision risk between Shell 2 and Shell 3, if a satellite in Shell 3 fails, there is no collision risk between the satellite and a satellite in Shell 2 before the malfunctioning satellite decays by more than 0.5 km; however, collision risk appears after that. If a satellite in Shell 2 fails, there is no collision risk between the satellite and satellites in Shell 3 because the operative satellite in Shell 3 is 30 km higher, which is larger than the sum of the orbital altitude variations of both satellites. The number of collisions between different shells is shown in Table 5.

4.2.4 Collision probability result

The number of malfunctioning satellites in each shell according to a malfunction rate of 1% is listed in Table 6.

The probability of more than one collision can be calculated as

$$P_{\geqslant 1} = 1 - P_0 = 1 - \mathrm{e}^{-\sum N} \tag{22}$$

where $\sum N$ is the total number of collisions caused by all malfunctioning satellites. The constellation's self-induced collision risks caused by each shell are listed in Table 7.

The effect of a single malfunctioning satellite on the safety of the constellation is related to the operating height of the satellite. The higher the orbital altitude, the greater the time of conjunctions with other normal satellites and the greater the collision probability. In addition, the collision risk is related to the number of satellites operating in a single shell. The larger the number, the more malfunctioning the satellites may be. In summary, Shell 3 has the greatest impact, with a collision probability caused by malfunctioning satellites of approximately 47.8%. This is followed by Shell 1, with a collision probability of approximately 45.1%. Shell 5, which deploys the smallest number of satellites, has the least impact, with a collision probability of approximately 12.5%. For the five shells near an altitude of 550 km in Phase 1, the total number of malfunctioning satellites is estimated to be 42, with a collision probability of 86.2%.

Table 5 Number of collisions of a single malfunctioning satellite with other operative satellites in different shells

Shell	Shell 1	Shell 2	Shell 3	Shell 4	Shell 5
Shell 1	—	0.016	0.005	0.004	0.002
Shell 2	0.012	—	0	0.002	0.001
Shell 3	0.033	0.040	—	0.005	0.003
Shell 4	0.022	0.028	0.010	—	0.003
Shell 5	0.022	0.028	0.010	0.005	—

Table 6 Number of malfunctioning satellites in Phase 1

Shell	Shell 1	Shell 2	Shell 3	Shell 4	Shell 5
Number of malfunctioning satellites	15	15	7	3	2

4.3 Comparison with collisions caused by objects outside the constellation

According to the results analyzed by Ren *et al.* [8], the collision probability between the Starlink constellation and catalogable objects (with sizes larger than 6 cm) in the external debris environment during the first five-year service period is shown in Table 8.

In Ren *et al.*'s study, Shells 4 and 5 were considered as one shell with a 97.6° inclination, and the collision probability of each shell subjected to external collision was calculated. According to the collision probability, the

Table 7 Self-induced collision risk caused by each shell

Shell	Collision caused by a single satellite	Collision probability caused by a single satellite	Collision caused by an entire shell	Collision probability caused by an entire shell (%)
Shell 1	0.040	0.039	0.600	45.1
Shell 2	0.007	0.027	0.390	32.3
Shell 3	0.093	0.089	0.651	47.8
Shell 4	0.068	0.066	0.204	18.5
Shell 5	0.067	0.065	0.134	12.5
Total	—	—	1.979	86.2

Table 8 Collision probability between the Starlink constellation and catalogable objects in the external debris environment during the first five years

Inclination (°)	53	53.2	70	97.6
Collision probability (%)	63.36	66.25	50.88	44.49

number of collisions can be determined using Eq. (20). During the five-year service period, the constellation may suffer from 3.39 external collisions, and the comprehensive collision probability is 96.6%, which is slightly higher than the 1.98 collisions and 86.2% collision probability caused by malfunctioning satellites inside the constellation. Collisions caused by malfunctioning satellites in the constellation are also important risk points that deserve significant attention.

5 Conclusions

The rapid deployment of the Starlink constellation may increase the risk of on-orbit collisions. The collision risk may be caused not only by space debris but also by satellites within the constellation. Focusing on the self-induced collision risk of the Starlink constellation caused by malfunctioning satellites, this paper presents a study of the conjunctions between a malfunctioning satellite and a satellite in the same or different orbital planes of the same shell based on long-term orbital evolution characteristics; furthermore, it analyzes the probability of collisions. Based on a malfunction rate of 1%, it is estimated that 42 satellites in all five shells of the Starlink constellation in the first phase will suddenly fail in orbit and become incapable of deorbiting in time. The malfunctioning satellite will cause 1.98 collisions with other satellites in all five shells, with a collision probability of approximately 86.2%, which is slightly lower than the probability of the constellation suffering from collisions caused by external detectable debris during the five-year service period. The results show that collisions caused by malfunctioning satellites in the constellation are also important risk points that deserve significant attention.

Declaration of competing interest

The authors have no competing interests to declare that are relevant to the content of this article.

References

[1] Space-Track website. Information on http://www.space-track.org (cited 1 Sep 2022)

[2] Kessler, D. J. Collisional cascading: The limits of population growth in low Earth orbit. *Advances in Space Research*, **1991**, 11(12): 63–66.

[3] Zhang, J., Cai, Y., Xue, C., Xue, Z., Cai, H. LEO mega constellations: Review of development, impact, surveillance, and governance. *Space*: *Science & Technology*, **2022**, 2022: 9865174.

[4] Yun, C., Hu, M., Song, Q., Wu, T. Security research and maneuver avoidance strategy of LEO constellation. *Space Debris Research*, **2020**, 20(3): 17–23. (in Chinese)

[5] United Nations Office for Outer Space Affairs. Information on https://www.unoosa.org/oosa/en/oosadoc/data/documents/2021/aac.105/aac.10512620.html (cited 1 Mar 2023)

[6] Radtke, J., Kebschull, C., Stoll, E. Interactions of the space debris environment with mega constellations—Using the example of the OneWeb constellation. *Acta Astronautica*, **2017**, 131: 55–68.

[7] Bastida Virgili, B., Dolado, J. C., Lewis, H. G., Radtke, J., Krag, H., Revelin, B., Cazaux, C., Colombo, C., Crowther, R., Metz, M. Risk to space sustainability from large constellations of satellites. *Acta Astronautica*, **2016**, 126: 154–162.

[8] Ren, S., Yang, X., Wang, R., Liu, S., Sun, X. The interaction between the LEO satellite constellation and the space debris environment. *Applied Sciences*, **2021**, 11(20): 9490.

[9] Le May, S., Gehly, S., Carter, B. A., Flegel, S. Space debris collision probability analysis for proposed global

broadband constellations. *Acta Astronautica*, **2018**, 151: 445–455.

[10] Lewis, H., Radtke, J., Beck, J., Virgili, B. B., Krag, H. Self-induced collision risk analysis for large constellations. In: Proceedings of the ESA/ESOC 7th European Conference on Space Debris, Darmstadt, Germany, **2017**: 7.

[11] Hu, S., Chen, L., Liu, L. The structure evolution of satellite constellation. *Acta Astronomica Sinica*, **2003**, 44(1): 46–54. (in Chinese)

[12] Chen, Y., Zhao, L., Liu, H., Li, L., Liu, J. Analysis of configuration and maintenance strategy of LEO walker constellation. *Journal of Astronautics*, **2019**, 40(11): 1296–1303. (in Chinese)

[13] Xiang, J., Fan, L., Zhang, Y. Study on design of the structure self-stabilization for satellite constellation. *Flight Dynamics*, **2007**, 25(4): 81–85. (in Chinese)

[14] Liu, L. *Orbital Theory of Spacecraft*. Beijing: National Defense Industry Press, **2000**: 126–136. (in Chinese)

[15] James, R. W. *Mission Geometry: Orbit and Constellation Design and Management*. Dordrecht, the Netherlands: Microcosm Press & Kluwer Academic Publishers, **2001**.

[16] Chobotov, V. A., Herman, D. E., Johnson, C. G. Collision and debris hazard assessment for a low-Earth-orbit space constellation. *Journal of Spacecraft and Rockets*, **1997**, 34(2): 233–238.

[17] Chen, L., Han, L., Bai, X. *Orbital Dynamics and Error Analysis of Space Object*. Beijing: National Defense Industry Press, **2011**.

[18] Klinkrad, H. *Space Debris: Models and Risk Analysis*. Berlin Heidelberg, Germany: Springer, **2006**.

Wei Zhang was born in 1986. He has a bachelor degree in electronic engineering and a master degree in computer science and technology from Peking University, China. He is currently a senior engineer at Xi'an Satellite Control Center. His research interests are focused in the fields of space surveillance and tracking, space objects catalogue, and space safety. E-mail: colagrape@163.com